Digital Subtraction Ductography

Johnson B. Lightfoote[1]
Richard M. Friedenberg
Michael F. Smolin

Digital subtraction techniques used in the examination of eight patients with salivary and nasolacrimal disease are described. Pleomorphic adenoma, ductal stricture, extrinsic masses, parotid-otic fistula, and a radiolucent calculus were demonstrated. The procedures are more easily performed than film techniques, and pathology is better demonstrated by digital ductography than on a film examination. Image subtraction, reregistration, and window manipulation allowed clear demonstration of ducts about the head and neck, overcoming limitations imposed by inherently high object contrast. Digital subtraction ductography is an important nonvascular application of digital imaging technology.

Digital video subtraction imaging has proven to be of value by providing improved contrast detectability coupled with the subtraction of overlying structures. Digital subtraction angiography has been used in the imaging of the vascular tree [1–3]. Nonvascular applications of digital subtraction radiography have recently been reported, such as digital subtraction laryngography [4]. We have used digital subtraction radiography to enhance the diagnostic capability of head and neck ductography, and here report our technique and results in digital dacryocystography (one patient) and digital sialography (seven patients). The procedures are easily performed, and are significantly superior in interpretability in comparison with traditional nonsubtraction film methods.

Materials and Methods

The theory and technology of digital video subtraction imaging has been described in detail [1]. Eight consecutive patients referred for evaluation of suspected salivary or nasolacrimal pathology were examined using digital techniques. Our patients were examined using a dedicated Xonics digital DR-20 system. A 9-inch (23-cm) image intensifier (6-inch [15-cm] and 4.5-inch [11-cm] field sizes also available) is coupled to an Amperex Plumbicon-based television camera. Analog-to-digital conversion is performed with 10 bits of resolution, and video images are stored in a 512 × 512 × 8-bit-deep memory. The system is based on a PDP LSI 11/23 computer and a 184 Mbyte disk; image acquisition protocol programming, mask/image reregistration, and video window control are among the available facilities.

For digital sialography, a 0 or 00 cannula was inserted into Stensen's duct, and meglumine iothalamate 60% (4–6 ml) was injected by hand. Video images were acquired at 1 frame/sec. The procedure was performed first in the lateral and then in the posteroanterior (PA) projection. Typical exposure values per frame were 90 kVp, 25 mAs. Each projections required a total of 10–25 frames per patient examined.

For dacryocystography, a 00 cannula was inserted into the punctum of the inferior canaliculus, and 4 ml of meglumine iothalamate was hand-injected. Digital image acquisition was performed in the PA projection at a 1/sec frame rate for a total of five exposures. Technical factors used were 99 kVp and 64 mAs.

Image selection, subtraction, and reregistration are performed by the radiologist. Hard-copy images are recorded by standard multiformat camera.

Radiation exposure of the lens of the eye was estimated using a standard phantom and an MDH IOI5C x-ray probe for both procedures.

Received June 18, 1984; accepted after revision September 27, 1984.

[1] All authors: Department of Radiological Sciences, University of California, Irvine Medical Center, 101 City Dr. S., Orange, CA 92668. Address reprint requests to J. B. Lightfoote.

AJR 144:635–638, March 1985
0361–803X/85/1443–0635

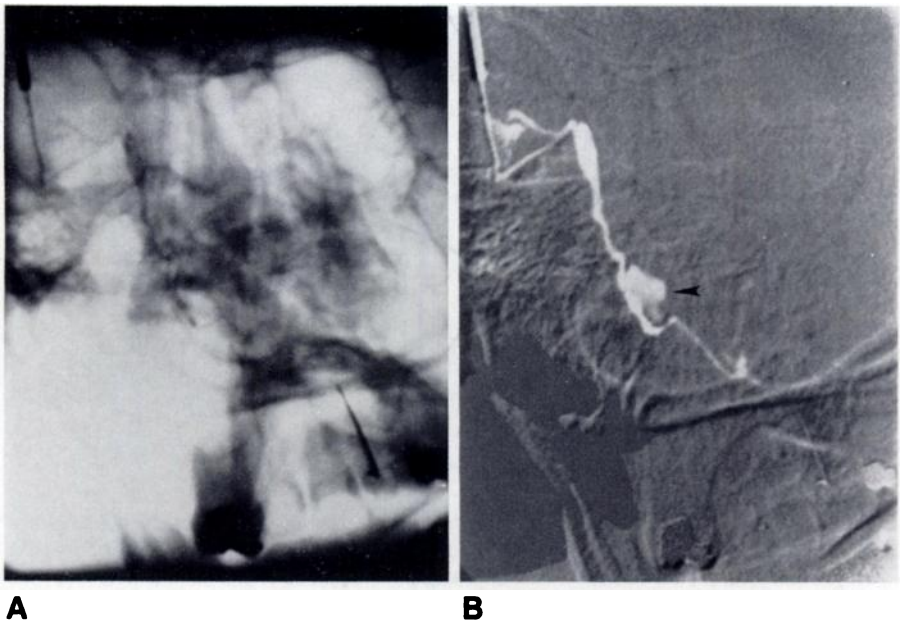

Fig. 1.—Case 1. **A,** Nonsubtracted video fluorographic image. Contrast material faintly seen in nasolacrimal duct. **B,** PA projection, digital subtraction dacryocystogram clearly demonstrates normal canaliculus, nasolacrimal duct, and spill of contrast into inferior turbinate (*arrowhead*). Small amount of contrast is seen in conjunctival sac.

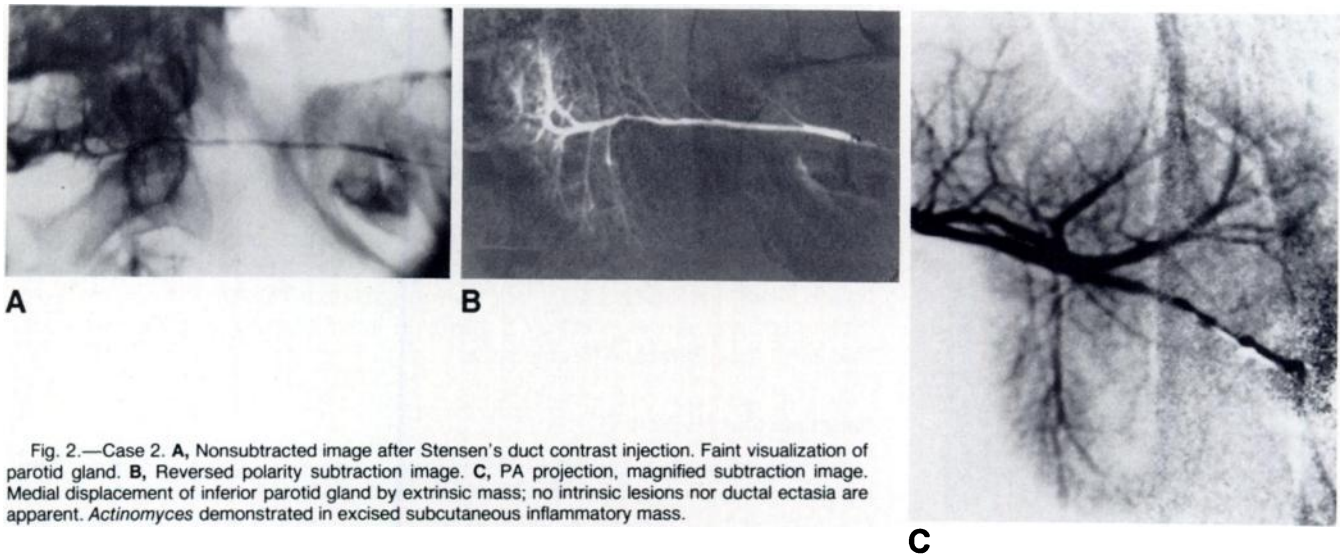

Fig. 2.—Case 2. **A,** Nonsubtracted image after Stensen's duct contrast injection. Faint visualization of parotid gland. **B,** Reversed polarity subtraction image. **C,** PA projection, magnified subtraction image. Medial displacement of inferior parotid gland by extrinsic mass; no intrinsic lesions nor ductal ectasia are apparent. *Actinomyces* demonstrated in excised subcutaneous inflammatory mass.

Representative Case Reports

Case 1

A 26-year-old woman complained of a watery right eye (epiphora). Corneal opacity in the opposite eye had diminished its visual acuity to 20/400; right-eye visual acuity was 20/60. No purulent discharge nor conjunctivitis was apparent. At the time of dacryocystography, cannulation of the inferior punctum was difficult because of a stricture. Digital dacryocystography (subtracted image) clearly demonstrated the canaliculus and nasolacrimal duct, patent beyond the tip of the probe, thus excluding a more peripheral obstructing lesion (fig. 1). Dilatation of the punctum with a no. 1 dilator resulted in resolution of the patient's epiphora.

Case 2

A 25-year-old woman complained of severe, painful, progressive swelling of the right face. She was febrile, and the right buccal and paramandibular area was edematous, indurated, erythematous, and extremely tender. Digital sialography demonstrated extrinsic mass displacement of the ducts and parenchyma of the right parotid gland (fig. 2). No intraglandular mass, ductal ectasia, ductal obstruction, calculi, filling defects, nor other evidence of intraglandular neoplasm or inflammation was seen. The right facial mass was surgically drained, and pathologic examination demonstrated *Actinomyces* infection, presumably originating from carious mandibular dentition.

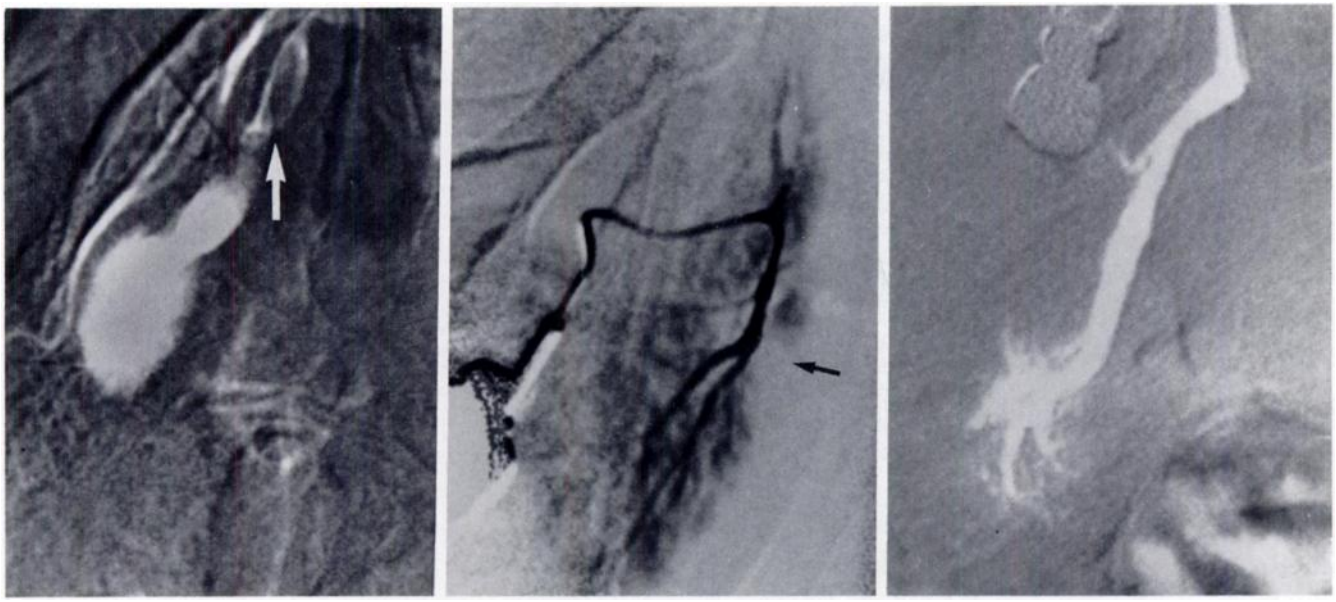

3 4 5

Fig. 3.—Case 5. Digital subtraction sialogram, verticosubmental projection. Radiolucent calculus partially obstructs Wharton's duct (*arrow*).

Fig. 4.—Case 3. PA subtraction image of parotid gland. Focal defect in parenchymal stain, consistent with fibrosis following excision of sebaceous adenoma (*arrow*).

Fig. 5.—Case 6. Digital subtraction sialogram, verticosubmental projection. Normal Wharton's duct and submandibular gland.

TABLE 1: **Digital Ductography Cases**

Case No. (age, gender)	Part Imaged	Findings
1 (26, F)	Right nasolacrimal duct	Punctum stricture
2 (25, F)	Right parotid gland	Extrinsic mass: *Actinomyces* abscess
3 (34, F)*	Left parotid gland	Extrinsic mass: infected sebaceous adenoma
4 (20, M)	Left parotid gland	Parotid-otic fistula
5 (36, F)	Left submandibular gland	Radiolucent staghorn calculus
6 (40, F)†	Left submandibular gland	Normal
7 (53, F)‡	Left parotid gland	Intrinsic mass: pleomorphic adenoma
8 (40, M)	Left parotid gland	Normal

* fig. 4.
† fig. 5.
‡ fig. 6.

Case 5

A 36-year-old woman complained of 18 months of recurrent intermittent left submandibular swelling. Digital radiography in the submentovertex projection demonstrated no calcification. Digital sialography of the submandibular gland demonstrated a 4 × 12 mm radiolucent filling defect in Wharton's duct; the acinar part of the gland was unremarkable (fig. 3). A staghorn calculus was removed at surgery.

Results

Of the eight patients examined, six demonstrated significant pathology; table 1 summarizes our experience.

Figure 1 demonstrates the significant improvement in duct and parenchymal visualization achieved by digital subtraction of postcontrast images from precontrast images and by video window level and width manipulation. Significant reregistration (as many as 7 pixels) was required to compensate for patient motion during the examination, and the availability of this function prevented the degradation of these studies into nondiagnostic ones. In fact, subtraction of bony and air-containing structures was often so complete as to obscure anatomic landmarks, and it was necessary to include unsubtracted or slightly misregistered images in archived hard copy to provide surgical landmarks.

Approximate examination time required for the eight cases was 15, 18, 20, 18, 18, 15, and 10 min for sialography, and 12 min for dacryocystography. These examination times include duct dilatation and cannulation, and compare favorably with our institution's experience with standard film technique procedure times.

Radiation exposure near the lens of the eye was 4.1 mR (1.06 μC/kg) in the posteroanterior projection, and 23.4 mR (6.04 μC/kg) in the lateral projection, per frame, for sialography. Lens exposure was 25.2 mR (6.50 μC/kg) in the PA projection for dacryocystography, per frame. These may be compared with the typical exposure associated with a single lateral skull radiograph of 240 mR (61.92 μC/kg), or with typical CT exposures of 1 R (258 μC/kg) [5].

Discussion

Angiographic application of digital subtraction technology is well documented, and extravascular application of digital

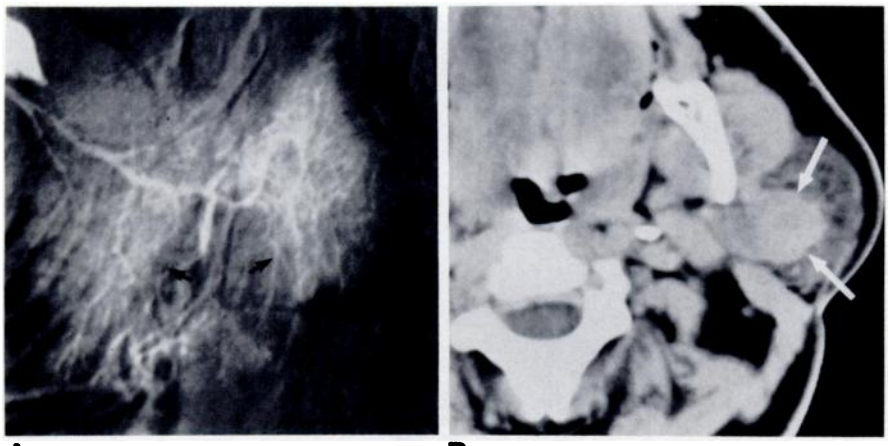

Fig. 6.—Case 7. **A,** Digital subtraction sialogram, lateral projection. **B,** CT scan. Intrinsic mass (*white arrows*) with displacement and stretching of left parotid parenchyma and ducts (*black arrows*). Pleomorphic adenoma removed at surgery.

radiography is now being explored. Object contrast in the head and neck is relatively great as compared with the rest of the body, owing to close apposition of bone and air-containing structures.

Routine imaging of the salivary gland and nasolacrimal system is made difficult by the high contrast between bone and air in the sinuses and pharynx, by overlapping structures, and by the very small size of the structures of interest [6–8]. Digital subtraction can effectively overcome the limitations imposed by high object contrast background structures. No attendant increase in radiation dose or procedure cost is incurred. In our experience, the examination quality is significantly superior by its subtraction of overlying background. Ducts and acinar detail are very clearly demonstrable. The examinations can be performed with somewhat greater facility and with some time savings by digital fluorography. The images are immediately available for review. Subtraction, reregistration, and window manipulation provide flexibility not available with film techniques. The L/U configuration of our dedicated digital system can achieve a projection such as verticosubmental easily.

The use of smaller doses of more dilute contrast media may reduce the frequency of sialographically-induced sialadenitis. The efficacy of CT imaging of the salivary glands has been demonstrated [9, 10]; digital subtraction imaging is simpler and faster and provides less radiation exposure.

Instillation of nonionic contrast agents (e.g., metrizamide) directly into the conjunctival sac has been previously shown to be nonirritating [11]. Such functional imaging of the nasolacrimal system could be exploited to advantage by digital subtraction technique [12].

Digital subtraction ductography of the salivary gland and nasolacrimal system provides significantly improved diagnostic imaging of these structures over routine sialography with savings in time, contrast dose, and radiation dose, and with greater flexibility in comparison with traditional film methods. Digital ductography is an important nonvascular application of digital subtraction imaging technology.

REFERENCES

1. Mistretta CA, Crummy AB, Strother CM. Digital angiography: a perspective. *Radiology* **1981**;139:273–276
2. Crummy AB, Stieghorst MF, Turski PA, et al. Digital subtraction angiography: current status and use of intra-arterial injection. *Radiology* **1982**;145:303–307
3. Riederer SJ, Kruger RA. Intravenous digital subtraction: a summary of recent developments. *Radiology* **1983**;147:633–638
4. Brown BM, Enzmann DR, Hopp ML, Castelino RA. Digital subtraction laryngography. *Radiology* **1983**;147:655–657
5. National Bureau of Standards. *Medical physics data book*. Washington, DC: U.S. Department of Commerce, **1982**:65
6. Adam EJ, Willson SA, Corcoran MO, Horsley M. The value of parotid sialography. *Br J Surg* **1983**;70:108–110
7. Del Balso AM, Williams E, Tane TT. Parotid masses: current modes of diagnostic imaging. *Oral Surg* **1982**;54:360–364
8. Golding S. Computed tomography in the diagnosis of parotid gland tumours. *Br J Radiol* **1982**;55:182–188
9. Bryan RN, Miller RH, Ferreyo RI, Sessions RB. Computed tomography of the major salivary glands. *AJR* **1982**;139:547–554
10. Carter BL, Karmody CS, Blickman JR, Panders AK. Computed tomography and sialography. 2. Pathology. *J Comput Assist Tomogr* **1981**;5:46–53
11. Johansen JG, Udnaes I. Dacryocystography with Amipaque (metrizamide). *Acta Ophthalmol* **1977**;55:637–683
12. Rosenstock T, Hurwitz JJ. Functional obstruction of the lacrimal drainage passages. *Can J Ophthalmol* **1982**;17:249–255